Metabolism 164 (2025) 156130

Contents lists available at ScienceDirect

Metabolism

journal homepage: www.journals.elsevier.com/metabolism

Subphenotypes of body composition and their association with cardiometabolic risk – Magnetic resonance imaging in a population-based sample

Elena Grune [a,b,c], Johanna Nattenmüller [a,d], Lena S. Kiefer [e,f], Jürgen Machann [g,h,i], Annette Peters [b,i,j,k], Fabian Bamberg [a], Christopher L. Schlett [a], Susanne Rospleszcz [a,b,*]

[a] Department of Diagnostic and Interventional Radiology, Medical Center, Faculty of Medicine, University of Freiburg, Freiburg, Germany
[b] Institute of Epidemiology, Helmholtz Munich, Neuherberg, Germany
[c] Pettenkofer School of Public Health, LMU Munich, Munich, Germany
[d] Institute for Radiology and Nuclear Medicine Hirslanden Clinic St. Anna, Lucerne, Switzerland
[e] Section on Experimental Radiology, Department of Diagnostic and Interventional Radiology, Eberhard Karls University of Tuebingen, Tuebingen, Germany
[f] Department of Nuclear Medicine and Clinical Molecular Imaging, Eberhard Karls University of Tuebingen, Tuebingen, Germany
[g] Section on Experimental Radiology, Department of Diagnostic and Interventional Radiology, University Hospital Tübingen, Tübingen, Germany
[h] Institute for Diabetes Research and Metabolic Diseases, Helmholtz Munich at the University of Tübingen, Tübingen, Germany
[i] German Center for Diabetes Research (DZD), Neuherberg, Germany
[j] Institute for Medical Information Processing, Biometry, and Epidemiology (IBE), Medical Faculty, Ludwig-Maximilians-Universität (LMU), Munich, Germany
[k] German Center for Cardiovascular Disease Research (DZHK), Munich Heart Alliance, Munich, Germany

ARTICLE INFO

Keywords:
Obesity
Body composition
Adipose tissue
Magnetic resonance imaging
Cardiometabolic risk
Clustering
Population-based

ABSTRACT

Background: For characterizing health states, fat distribution is more informative than overall body size. We used population-based whole-body magnetic resonance imaging (MRI) to identify distinct body composition subphenotypes and characterize associations with cardiovascular disease (CVD) risk.
Methods: Bone marrow, visceral, subcutaneous, cardiac, renal, hepatic, skeletal muscle and pancreatic adipose tissue were measured by MRI in $n = 299$ individuals from the population-based KORA cohort. Body composition subphenotypes were identified by data-driven k-means clustering. CVD risk was calculated by established scores.
Results: We identified five body composition subphenotypes, which differed substantially in CVD risk factor distribution and CVD risk. Compared to reference subphenotype I with favorable risk profile, two high-risk phenotypes, III&V, had a 3.8-fold increased CVD risk. High-risk subphenotype III had increased bone marrow and skeletal muscle fat (26.3 % vs 11.4 % in subphenotype I), indicating ageing effects, whereas subphenotype V showed overall high fat contents, and particularly elevated pancreatic fat (25.0 % vs 3.7 % in subphenotype I), indicating metabolic impairment. Subphenotype II had a 2.7-fold increased CVD risk, and an unfavorable fat distribution, probably smoking-related, while BMI was only slightly elevated. Subphenotype IV had a 2.8-fold increased CVD risk with comparably young individuals, who showed high blood pressure and hepatic fat (17.7 % vs 3.0 % in subphenotype I).
Conclusions: Whole-body MRI can identify distinct body composition subphenotypes associated with different degrees of cardiometabolic risk. Body composition profiling may enable a more comprehensive risk assessment than individual fat compartments, with potential benefits for individualized prevention.

Abbreviations: AT, adipose tissue; BMAT, bone marrow adipose tissue; BMI, body mass index; CHD, coronary heart disease; CI, confidence interval; CVD, cardiovascular disease; eGFR, estimated glomerular filtration rate; EPCAT, epicardial adipose tissue; FRS, Framingham Risk Score; HbA1c, haemoglobin-A1c; HDL, high-density lipoprotein; LDL, low-density lipoprotein; MRI, magnetic resonance imaging; OR, odds ratio; PCAT, paracradial adipose tissue; PFF, pancreatic fat fraction; RFF, renal fat fraction; RSFF, renal sinus fat fraction; SAT, subcutaneous adipose tissue; SMFF, skeletal muscle fat fraction; T2D, type 2 diabetes mellitus; VAT, visceral adipose tissue.

* Corresponding author at: Universitätsklinikum Freiburg, Klinik für Diagnostische und Interventionelle Radiologie, Killianstr. 5a, 79106 Freiburg, Germany.
E-mail address: susanne.rospleszcz@uniklinik-freiburg.de (S. Rospleszcz).

https://doi.org/10.1016/j.metabol.2024.156130
Received 1 October 2024; Accepted 27 December 2024
Available online 30 December 2024

1. Introduction

Obesity is a major risk factor for chronic diseases, such as cardiovascular disease (CVD) or diabetes, and is associated with an increased risk for certain cancers. With over 1 billion people affected and a steadily increasing prevalence in recent decades, obesity is one of the biggest healthcare problems worldwide [1].

The development of obesity is multifactorial, with genetic, environmental, social and behavioral factors contributing to it. In general, it is characterized by an excessive accumulation of adipose tissue (AT) in various body compartments but in clinical practice, the definition is commonly based on anthropometric measures such as body mass index (BMI) or waist circumference [2]. These metrics are easy to determine; however, they do not reflect the true amount and distribution of AT in the body at individual level and therefore only serve as a surrogate measure [3].

The need to characterize body composition beyond anthropometric measures has been recognized. It is established that different abdominal and ectopic fat depots are metabolically active to different degrees, and thus differ in possible unfavorable health effects [4]. Moreover, individuals with normal BMI can still present with high ectopic fat contents, which might place them at higher metabolic risk without being overweight [5]. Abdominal visceral (VAT) and subcutaneous adipose tissue (SAT) have received particular attention, as they have key metabolic functions in energy homeostasis and glucose regulation. Especially VAT is secreting higher levels of cytokines and adipokines compared to SAT and contributes to chronic low-grade inflammation and disrupting insulin sensitivity [6,7]. Further, VAT is associated with various adverse cardiometabolic outcomes, whereas the role of SAT in cardiometabolic risk is still controversial [8,9].

Ectopic fat in bone marrow, heart, kidneys, liver, skeletal muscles or pancreas have local and systemic effects, but their exact role in cardiometabolic risk is less established [10]. Hepatic steatosis has been linked to hypertension, dyslipidemia and impaired glucose metabolism [11,12]. Studies examining pancreatic fat pointed towards an association with the metabolic syndrome, but results on the relation to type 2 diabetes (T2D) remained ambiguous [13,14]. Fat infiltration in the skeletal muscle, which plays a major role in insulin-stimulated glucose uptake, has been related to insulin resistance [15]. Bone marrow AT was associated with dyslipidemia, and might be increased in T2D patients [16,17].

Taken together, it is important to investigate not only single AT depots in isolation, but also their interplay and clustering to learn about potential high-risk phenotypes of body composition. First studies have demonstrated that body composition profiling based on medical imaging identifies fat distribution phenotypes and different associated risk factor profiles [18,19].

For the quantification of AT, magnetic resonance imaging (MRI) is an accurate, reliable and non-invasive method, making it the gold standard in body composition profiling.

In this study, we derived a large panel of AT depots by whole-body MRI in a sample from a population-based cohort. Our aims were threefold: 1) to characterize the association of different AT depots with estimated cardiometabolic risk and individual risk factors, 2) to identify subphenotypes of body composition by data-driven clustering on AT depots, and 3) to characterize associations of body composition subphenotypes with cardiometabolic risk and risk factors.

2. Methods

2.1. Study population

We used data from the KORA-MRI study conducted in 2013–2014, a cross-sectional subsample from the KORA-FF4 survey ("Cooperative Health Research in the Region Augsburg"). The FF4 study ($n = 2279$) is the second follow-up of the original population-based survey KORA-S4 ($n = 4261$, enrolled in 1999–2001). Details on design, sampling procedure and data collection of the KORA studies are described elsewhere [20].

In KORA-MRI, 400 participants aged between 39 and 73 years underwent whole-body MRI [21]. The included individuals had no prior history of validated/self-reported stroke, myocardial infarction, or revascularization and did not have impaired renal function or any MRI contraindication. As a main aim of the study was to assess subclinical disease across the glycemic spectrum, it comprised a high proportion of participants with prediabetes (26 %) and diabetes (14 %). The MRI exam took place within three months after the initial visit at the study center [21].

The KORA studies are approved by the Ethics committee of the Bavarian Chamber of Physicians (EC No.06068). The Ethics Committee of the LMU additionally approved the MRI examination (No. 498–12). All participants gave written informed consent. The study has been conducted according to the Declaration of Helsinki.

2.2. Body composition assessment by MRI

Whole-body MRI scans were performed on a 3 Tesla Magnetom Skyra (Siemens AG, Healthcare Sector, Erlangen, Germany) equipped with an 18-channel body coiling system. The examination comprised sequences to cover brain, cardiovascular system, and AT compartments of the chest and abdomen as previously described in detail (Supplementary Text 1, [21]).

Hepatic steatosis was defined as hepatic fat fraction at portal vein (HFF pv) $\geq$5.75 % [22]. Pancreatic steatosis was defined as fat fraction in the pancreatic body (PFF cor) $\geq$6.2 % [23].

2.3. Risk factor assessment

During their visit at the study center, all participants underwent standardized physical examinations. A fasted blood sample was taken and trained personnel conducted face-to-face interviews. The collection of clinical data has been described previously [20].

Briefly, BMI was defined as weight (kilograms) divided by the height squared (square meters). Overweight was defined as BMI $\geq$25 kg/m^2 and $<$ 30 kg/m^2, obesity as BMI $\geq$30 kg/m^2. Systolic and diastolic blood pressure were measured three times on the right arm after at least 5 min of rest. The mean of the second and third measurement were considered for the present analysis. Hypertension was defined as systolic blood pressure of at least 140 mmHg, diastolic blood pressure of at least 90 mmHg or receiving antihypertensive treatment, while being aware of having hypertension.

Participants without prior T2D diagnosis were administered an oral glucose tolerance test. The glycemic status was categorized into normoglycemic, prediabetes or diabetes according to WHO guidelines [24]. Further, haemoglobin-A1c (HbA1c), high sensitivity C-reactive protein concentration (hsCRP), total cholesterol, high-density lipoprotein (HDL), low-density lipoprotein (LDL), triglycerides, and estimated glomerular filtration rate (eGFR) were measured by standard laboratory techniques [25]. Dyslipidemia was defined as LDL $\geq$130 mg/dL or intake of lipid-lowering medication.

Cigarette and alcohol consumption, regular physical activity, and intake of antihypertensive, antidiabetic or lipid-lowering medication were self-reported. Physical activity was assessed by weekly leisure-time sports in summer and winter, categorized as: (1) >2 h, (2) 1–2 h, (3) <1 h, and (4) none. The total score, summing both seasons, classified participants as physically inactive (score $\geq$ 5) or physically active (score $<$ 5).

For women, postmenopause was defined if women reported no menses for >12 consecutive months, had a hysterectomy with or without bilateral oophorectomy, or were older than 60 years.

In addition to MRI-based assessment of body composition, whole-body bioelectrical-impedance analysis was used to quantify total body

fat mass, lean body mass and appendicular muscle mass [26]. Skeletal muscle mass was calculated as (body height^2/resistance) × 0.401 + (gender × 3.825) + (age × 0.071) + 5.102 (body height in cm, resistance in Ω, gender male = 1, female = 0, age is in years) as derived in [27]. All BIA measures are presented as indices normalized to participants' body height squared.

2.4. CVD risk assessment

To estimate CVD risk, we calculated three well-established risk scores (SCORE2, FRS 10 years, FRS 30 years) [28–31]. All risk scores include age, sex, systolic blood pressure, smoking status, HDL, total cholesterol and T2D. Antihypertensive treatment is a covariate in all models but SCORE2. Since none of the study participants had prior CVD, risk scores were calculated for all individuals.

In the extended SCORE2-Diabetes algorithm, the model was adapted for use in individuals with diabetes incorporating age at diabetes diagnosis, HbA1c and eGFR as additional risk factors and the same endpoint definition.

The Framingham Risk Score (FRS 10 years) estimates the 10 years risk for coronary heart disease (CHD), cerebrovascular events, peripheral artery disease, and heart failure. We calculated the score according to the published formula with recalibration for the sample at hand.

The 30-year Framingham Risk Score (FRS 30 years) predicts the 30-year risk of hard CHD, fatal or nonfatal stroke. We computed the risk based on the original equations [32].

2.5. Identification of body composition subphenotypes

Unsupervised k-means clustering using the Hartigan-Wong algorithm was applied to derive clusters representing subphenotypes of body composition. Conceptually, participants within one cluster should be similar to each other regarding their fat distribution and different from individuals in other clusters. AT data were standardized by subtracting their mean and dividing by their standard deviation, stratified by sex. The number of clusters k was determined by majority vote of 23 indices implemented in the R package NbClust (Supplementary Text 2). Cluster stability was assessed by repeating the clustering on 100 bootstrap samples and calculating the Jaccard index, which quantifies the similarity between the original clusters and the bootstrapped ones (Supplementary Text 3). A visual validation of cluster separation was performed using a scatterplot of the first two principal component coordinates.

Different sensitivity analyses were conducted. First, clusters were recalculated by hierarchical clustering. Second, a different variable set with aggregated measures (mean values of the fat content in each of the 8 depots) was used for k-means clustering (Supplementary Text 4). In both cases, stability was assessed and compared to the final k-means clustering.

2.6. Statistical methods

AT data, risk factors and risk scores are given as mean and standard deviation or median and interquartile range for continuous variables and as count and percentage for categorical variables. Differences between groups were assessed by one-way ANOVA and X^2-test, respectively. Correlations between AT depots, risk factors and estimated risk scores were determined by Spearman's rho correlation coefficient and corresponding *p*-values.

To evaluate the association between single AT compartments as exposures and risk factors as outcomes, linear or logistic regression models adjusted for age and sex were fit. Estimates are reported as beta coefficients or odds ratios (OR) with corresponding 95 % confidence intervals (CIs). AT parameters were standardized before modeling. To evaluate the association between single AT compartments as exposures and CVD risk scores as outcomes, risk scores were log transformed prior to linear regression analysis due to their skewed distribution. Since risk score calculation included age and sex, these regression models were unadjusted. Estimates are reported as exponentiated beta coefficients, corresponding to percent change in geometric mean.

The distribution of AT compartments across clusters representing subphenotypes of body composition was graphically illustrated by radar charts. To assess the association of subphenotypes with risk factors and risk scores, linear and logistic regression models analogous to the ones described above were calculated. We emphasize that these models are used for evaluating associations, and not for dedicated statistical prediction.

P-values <0.05 were considered to indicate statistical significance. All analyses were conducted with R (version 4.3.3).

3. Results

3.1. Study sample

The final sample comprised $n = 299$ individuals (mean age 56.5 ± 9.1 years, 41.1 % women, Table 1). One person had retroactively withdrawn consent for data usage, and individuals with missing values in any of the AT data were excluded, as illustrated in Fig. 1. Missing values in AT data were due to poor image quality, image artefacts or technical malfunctions and therefore assumed to be missing at random. Comparing the 299 participants in the final sample with individuals who had been excluded due to missing AT data, there were no significant differences in anthropometric or risk factor data (Supplementary Table 1).

In the final sample, participants had a mean BMI of 28.1 kg/m^2, the prevalence of hypertension was 33.8 % and of diabetes 13.4 % (Table 1). Average CVD risk within 10 years as estimated by SCORE2 was 6.0 %.

AT data showed significant differences between men and women except for bone marrow fat (BMAT), and fat in the psoas major (SMFF pm) and quadratus lumborum (SMFF ql) muscles (Table 2).

3.2. Correlations between adipose tissue compartments, risk factors and estimated CVD risk

AT compartments, risk factors and estimated CVD risk were correlated to different degrees (Supplementary Fig. 1). Notably, the strongest positive correlation between the different AT compartments was found between VAT and HFF pv (Spearman's rho = 0.78, $p < 0.001$), whereas BMAT and EPCAT showed the weakest significant correlation ($r = 0.15$, $p < 0.001$). BMI was strongly correlated with SAT ($r = 0.80$, $p < 0.001$). Correlation between the risk scores was high and exceeded 0.92 in each case; VAT showed the strongest correlation with risk scores (e.g. $r = 0.63$, $p < 0.001$ for FRS 30).

3.3. Associations between adipose tissue compartments and risk factors

AT compartments were associated with cardiometabolic risk factors (Supplementary Fig. 2). For outcomes hypertension, systolic and diastolic blood pressure, largest effect sizes were found for VAT (OR = 1.98, 95%CI = [1.49, 2.68], $p < 0.001$, β = 3.93 mmHg, [2.24, 5.61], $p < 0.001$, and β = 2.67 mmHg, [1.58, 3.76], $p < 0.001$, respectively). Regarding lipid profile, strongest associations with total and LDL cholesterol were seen for BMAT (β = 8.80 mg/dL, [4.24, 13.37], $p < 0.001$, and β = 6.65 mg/dL, [2.52, 10.77], $p = 0.002$, respectively). For outcome diabetes, we found the largest effect size for HFF lobe (OR = 2.31, [1.65, 3.30], $p < 0.001$. All AT compartments except BMAT were significantly associated with BMI, with SAT showing the largest effect (β = 3.93 kg/m^2, [3.69, 4.18], $p < 0.001$). These observations were confirmed by the distribution of BMAT and SAT, respectively, according to BMI (Supplementary Fig. 3). Moreover, variability of hepatic and pancreatic AT increased considerably with increasing BMI (Supplementary Fig. 3).

Table 1
Characteristics of the study sample.

	All	Men	Women	
	N = 299	*N* = 176 (59.9 %)	*N* = 123 (41.1 %)	p-value
Age, years	56.5 ± 9.1	56.3 ± 9.2	56.7 ± 9.1	0.744
Postmenopausal	–	–	74 (60.2 %)	–
Anthropometrics				
Weight, kg	82.9 ± 15.3	89.5 ± 12.8	73.4 ± 13.6	<0.001
BMI, kg/m^2	28.1 ± 4.5	28.4 ± 3.9	27.7 ± 5.2	0.193
BMI categories				0.002
Normal-weight	74 (24.7 %)	32 (18.2 %)	42 (34.1 %)	
Overweight	135 (45.2 %)	92 (52.3 %)	43 (35.0 %)	
Obesity	90 (30.1 %)	52 (29.5 %)	38 (30.9 %)	
Waist-To-Hip-Ratio	0.9 ± 0.1	1.0 ± 0.1	0.9 ± 0.1	<0.001
Hepatic steatosis	130 (43.5 %)	95 (54.0 %)	35 (28.5 %)	<0.001
Pancreatic steatosis	140 (46.8 %	90 (51.1 %)	50 (40.7 %)	0.095
Blood Pressure				
Systolic Blood Pressure, mmHg	121.1 ± 16.1	126.3 ± 15.3	113.6 ± 14.3	<0.001
Diastolic Blood Pressure, mmHg	75.6 ± 9.6	77.8 ± 9.	72.4 ± 8.5	<0.001
Hypertension	101 (33.8 %)	66 (37.5 %)	35 (28.5 %)	0.133
Antihypertensive Medication	72 (24.1 %)	39 (22.2 %)	33 (26.8 %)	0.428
Glycemia				0.026
Normoglycemia	184 (61.5 %)	100 (56.8 %)	84 (68.3 %)	
Prediabetes	75 (25.1 %)	45 (25.6 %)	30 (24.4 %)	
Diabetes	40 (13.4 %)	31 (17.6 %)	9 (7.3 %)	
HbA1c, %	5.6 ± 0.8	5.6 ± 0.9	5.6 ± 0.5	0.598
Antidiabetic Medication	23 (7.7 %)	15 (8.5 %)	8 (6.5 %)	0.672
Lipid Profile				
Total Cholesterol, mg/dL	218.4 ± 36.6	216.6 ± 38.4	221.0 ± 34.0	0.314
HDL Cholesterol, mg/dL	61.1 ± 17.5	55.3 ± 15.1	69.5 ± 17.4	<0.001
LDL Cholesterol, mg/dL	141.0 ± 32.7	142.5 ± 33.5	139.0 ± 31.6	0.368
Triglycerides, mg/dL	133.8 ± 88.8	154.2 ± 105.2	104.5 ± 43.6	<0.001
Lipid-lowering Medication	32 (10.7 %)	19 (10.8 %)	13 (10.6 %)	1.000
Dyslipidemia	208 (69.6 %)	127 (72.2 %)	81 (65.9 %)	0.299
Other laboratory markers				
hsCRP, mg/dL	1.1 [0.6, 2.4]	1.1 [0.6, 2.3]	1.3 [0.7, 2.8]	0.359
eGFR, ml/min/1.73 m^2	90.1 ± 14.0	91.4 ± 13.8	88.2 ± 14.1	0.054
Lifestyle				
Smoking				0.352
Never smoker	111 (37.1 %)	61 (34.7 %)	50 (40.7 %)	
Ex-smoker	129 (43.1 %)	82 (46.6 %)	47 (38.2 %)	
Smoker	59 (19.7 %)	33 (18.8 %)	26 (21.1 %)	
Alcohol consumption, g/day	18.1 ± 22.3	25.1 ± 25.1	8.1 ± 11.6	<0.001
Regular physical activity	177 (59.2 %)	101 (57.4 %)	76 (61.8 %)	0.52
BIA				
Total body fat mass index, kg/m^2	9.2 ± 3.1	8.3 ± 2.4	10.6 ± 3.4	<0.001
Lean body mass index, kg/m^2	18.9 ± 2.4	20.1 ± 1.8	17.1 ± 2.1	<0.001
Appendicular muscle mass index, kg/m^2	7.9 ± 1.4	8.6 ± 0.8	6.9 ± 0.9	<0.001
Skeletal muscle mass index, kg/m^2	9.3 ± 1.6	10.4 ± 1.0	7.8 ± 0.9	<0.001
Estimated CVD risk				
SCORE2, %	6.0 ± 4.7	7.4 ± 5.0	3.9 ± 3.4	<0.001
FRS 10 years, %	11.4 ± 10.5	14.6 ± 11.7	6.9 ± 6.3	<0.001
FRS 30 years, %	39.8 ± 19.4	45.9 ± 18.8	31.1 ± 16.9	<0.001

Values are given as mean ± SD or median [IQR] for continuous values and counts (percentage) for categorical values. P-values from t-test or X^2 test, respectively. Abbreviations. BMI: Body mass index, hsCRP: high-sensitivity C-reactive protein, HDL: high-density lipoprotein, LDL: low-density lipoprotein, eGFR: estimated glomerular filtration rate, BIA: bioelectrical-impedance analysis, CVD: cardiovascular disease, SCORE2: Systematic Coronary Risk Evaluation Model 2, FRS: Framingham Risk Score.

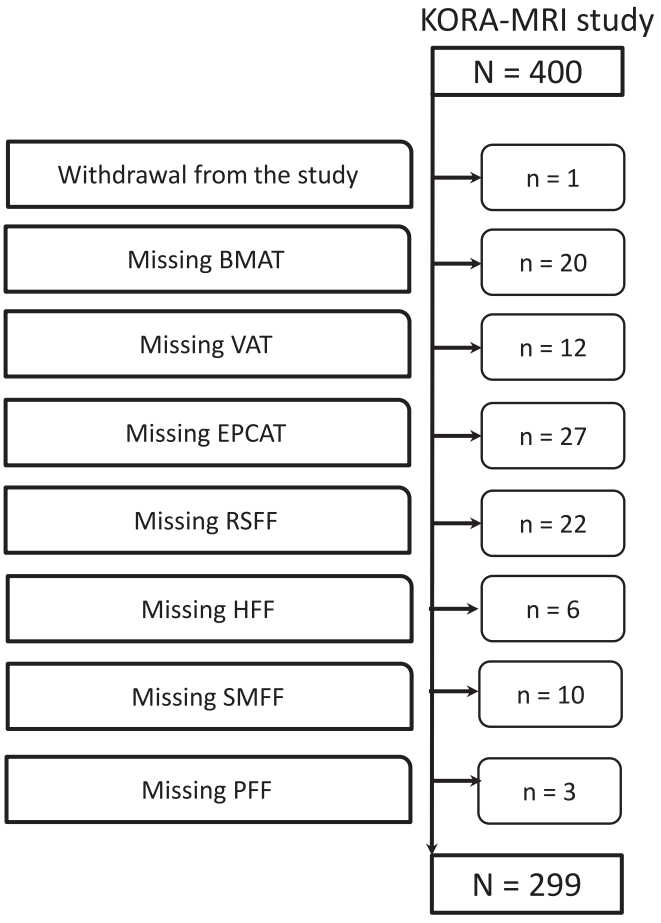

Fig. 1. Participant flowchart.
Abbreviations: BMAT: bone marrow adipose tissue, VAT: visceral adipose tissue, EPCAT: epicardial adipose tissue, RSFF: renal sinus fat fraction, HFF: hepatic fat fraction, SMFF: skeletal muscle fat fraction, PFF: pancreatic fat fraction.

Table 2
MRI-derived adipose tissue compartments in the study sample.

	All	Men	Women	
	N = 299	N = 176	N = 123	p-value
BMAT L1, %	52.9 ± 10.4	52.7 ± 10.1	53.1 ± 11.0	0.76
BMAT L2, %	56.5 ± 10.5	56.5 ± 9.9	56.3 ± 11.2	0.86
VAT, L	4.6 ± 2.7	5.8 ± 2.5	3.0 ± 1.8	<0.001
SAT, L	8.1 ± 3.4	7.4 ± 3.0	9.1 ± 3.8	<0.001
EPCAT, cm^2	9.0 ± 4.7	10.3 ± 5.0	7.2 ± 3.4	<0.001
PCAT, cm^2	21.1 ± 13.7	27.0 ± 14.4	12.7 ± 6.5	<0.001
RSFF, %	64.2 ± 10.0	67.6 ± 7.0	59.3 ± 11.4	<0.001
RFF, %	7.9 ± 3.2	8.8 ± 3.0	6.5 ± 3.0	<0.001
HFF lobe, %	8.8 ± 7.7	10.6 ± 8.3	6.2 ± 6.0	<0.001
HFF pv, %	8.5 ± 8.4	10.1 ± 8.5	6.3 ± 7.8	<0.001
SMFF pm, %	7.5 ± 3.3	7.4 ± 3.1	7.5 ± 3.6	0.85
SMFF ql, %	6.8 ± 3.8	6.4 ± 3.5	7.3 ± 4.2	0.062
SMFF ra, %	15.1 ± 9.8	13.2 ± 8.5	17.8 ± 10.9	<0.001
SMFF ab, %	17.4 ± 7.8	15.3 ± 6.9	20.5 ± 7.9	<0.001
PFF cap, %	8.0 ± 7.6	9.3 ± 8.8	6.1 ± 5.2	<0.001
PFF cor, %	8.1 ± 7.5	9.2 ± 8.5	6.5 ± 5.3	0.001
PFF cau, %	7.8 ± 7.3	8.8 ± 8.0	6.5 ± 5.9	0.006

Values are given as mean ± SD with *p*-values from *t*-test. Abbreviations: BMAT L1/L2: bone marrow adipose tissue at vertebrae L1/L2, VAT: visceral adipose tissue, SAT: subcutaneous adipose tissue, EPCAT: epicardial adipose tissue, PCAT: paracardial adipose tissue, RSFF: renal sinus fat fraction, RFF: renal fat fraction, HFF lobe/pv: hepatic fat fraction at right and left lobe or portal vein, SMFF pm/ql/ra/ab: skeletal muscle fat fraction of psoas major/quadratus lumborum/rectus abdominis/autochthonous back muscles, PFF cap/cor/cau: pancreatic fat fraction at caput/corpus/cauda.

3.4. Associations between adipose tissue compartments and estimated CVD risk

Overall, AT compartments VAT, SMFF ab, and BMAT showed the strongest associations with estimated CVD risk (Fig. 2). One SD increase in VAT was associated with a 50 % [38 %, 64 %] increase in geometric mean of FRS10 and a 33 % [26 %, 41 %] increase in FRS30. One SD increase in SMFF ab was associated with a 57 % [44 %, 72 %] increase in geometric mean of SCORE2. Overall, increase of any AT compartment was significantly associated with increasing risk scores.

3.5. Identification of body composition subphenotypes

AT depots listed in Table 2 were used for clustering. The final number of clusters was k = 5 based on majority vote of all indices (Supplementary Text 2). Clusters showed good stability ranging from Jaccard Indices 0.63 to 0.85 (Supplementary Table 2). Stability of the final clustering was superior to the hierarchical clustering or clustering on aggregated data, which were done as sensitivity analysis (Supplementary Table 3). The visualization of clusters on the first two principal components depicted an appropriate separation of the data (Supplementary Fig. 4). Clusters were labeled with Roman numerals I to V, sorted according to average VAT.

The distribution of AT differed notably between the clusters (Fig. 3, Supplementary Fig. 5). Cluster I was characterized by overall low values in all AT compartments. In cluster II, levels of all AT compartments corresponded to the average values of the entire sample, except for BMAT, which was remarkably elevated (mean BMAT L1 in cluster I 40.8 %, in cluster II 56.1 %, Supplementary Table 5). In cluster III, all AT compartments were again elevated compared to cluster II. In particular, skeletal muscle and bone marrow fat, were highest in cluster III among all clusters (e.g. SMFF ab 26.3 %, BMAT L1 60.5 %). Cluster IV was characterized by highest SAT and liver fat (SAT 11.2 l, HFF lobe 17.2 %) among all clusters, whereas BMAT and muscle fat were lower than in cluster III or II. In cluster V, levels of all ATs were elevated, however most strikingly those of pancreatic fat (PFF cap 25.0 %). Variation in VAT was highest in clusters III and IV (Supplementary Table 5). Overall, the same patterns were observed when evaluating the clusters separately for men and women. However, elevation of muscle fat in cluster III was even more pronounced in women, whereas VAT was not elevated (Supplementary Fig. 6).

3.6. Associations between subphenotypes and risk factors

Cluster I had the most favorable cardiometabolic risk profile, since individuals were on average the youngest (mean age 48.5 years, Supplementary Table 4), had the lowest BMI (25.0 kg/m^2) and systolic blood pressure (113.3 mmHg), and were predominantly normoglycemic (88.9 %). In cluster II, all risk factors were elevated compared to cluster I, although BMI was only slightly higher (26.6 kg/m^2). We note that the proportion of active smokers was highest in cluster II (26.9 %). Cluster III comprised the oldest participants on average (63.1 years) with the highest total cholesterol levels (224.9 mg/dL), and the lowest proportion of physical activity (46.9 %). Cluster IV, comparably young on average (55.3 years), showed the highest BMI (32.0 kg/m^2), systolic blood pressure (128.9 mmHg), and together with cluster V the highest proportion of prediabetes and diabetes (64.6 %). Cluster V showed an overall unfavorable cardiometabolic risk profile, and notably comprised the highest amount of participants on medication (antihypertensive, glucose-lowering, lipid-lowering, Supplementary Table 4).

In line with these descriptive statistics, for risk factors as outcomes in regression models, (Supplementary Fig. 7), cluster II only showed moderate associations with BMI compared to cluster I (reference category): β = 2.11 kg/m2, 95%CI = [0.88, 3.34], $p < 0.001$, Supplementary Fig. 7K. Cluster III was associated with an increase in total cholesterol compared to cluster I (β = 16.5 mg/dL, [0.96, 32.0], $p = 0.037$, Supplementary Fig. 7D), and cluster IV with the highest increase in systolic and diastolic blood pressure (β = 11.5 mmHg, [6.16, 16.9], $p < 0.001$, and β = 9.3 mmHg, [5.80, 12.7], $p < 0.001$, respectively, Supplementary Fig. 7B,C). Regarding outcome HbA1c, the largest effect size was seen for cluster V with an increase of 0.58 % compared to cluster I (β = 0.58 %, [0.23, 0.93], $p = 0.001$, Supplementary Fig. 7H).

3.7. Associations between subphenotypes and estimated CVD risk

Subphenotypes showed distinct distributions of cardiovascular risk, as estimated by risk scores (Fig. 4A). Although cluster I showed lowest estimated risk for all scores (e.g. mean SCORE2 2.5 %, Supplementary Table 4), and cluster 5 showed highest estimated risk (e.g. SCORE2 8.3 %), there was no strictly gradual relationship: Risk in clusters II and IV was comparable, and risk in cluster III was almost as high as in cluster V. Regression models (Fig. 4B) supported these descriptive results: cluster II had a 2.7-times higher SCORE2 compared to cluster I (β = 2.66, 95% CI = [2.09, 3.40], $p < 0.001$). In cluster III and V, SCORE2 was 3.8-times higher than in cluster I (β = 3.79, [2.83, 5.08], $p < 0.001$, and β = 3.83, [2.73, 5.37], $p < 0.001$, respectively). For cluster IV an increase by 2.8-times was found (β = 2.75, [2.05, 3.69], $p < 0.001$). Again, we emphasize that these results reflect associations, and are not statistical predictions.

4. Discussion

Using a subsample from a population-based cohort, we identified body composition patterns based on a broad panel of abdominal and ectopic AT compartments measured by whole-body MRI, and evaluated their association with cardiometabolic risk as quantified by individual risk factors and risk scores.

Our findings are threefold. First, AT depots were related to cardiometabolic risk to different degrees. The strongest association with overall CVD risk was found for VAT, BMAT, and fat in the autochthonous back muscles. Second, data-driven clustering identified five distinct subphenotypes of body composition, which were characterized by different distributions of AT. Third, we found that subphenotypes exhibited different degrees of risk. Notably, we identified a

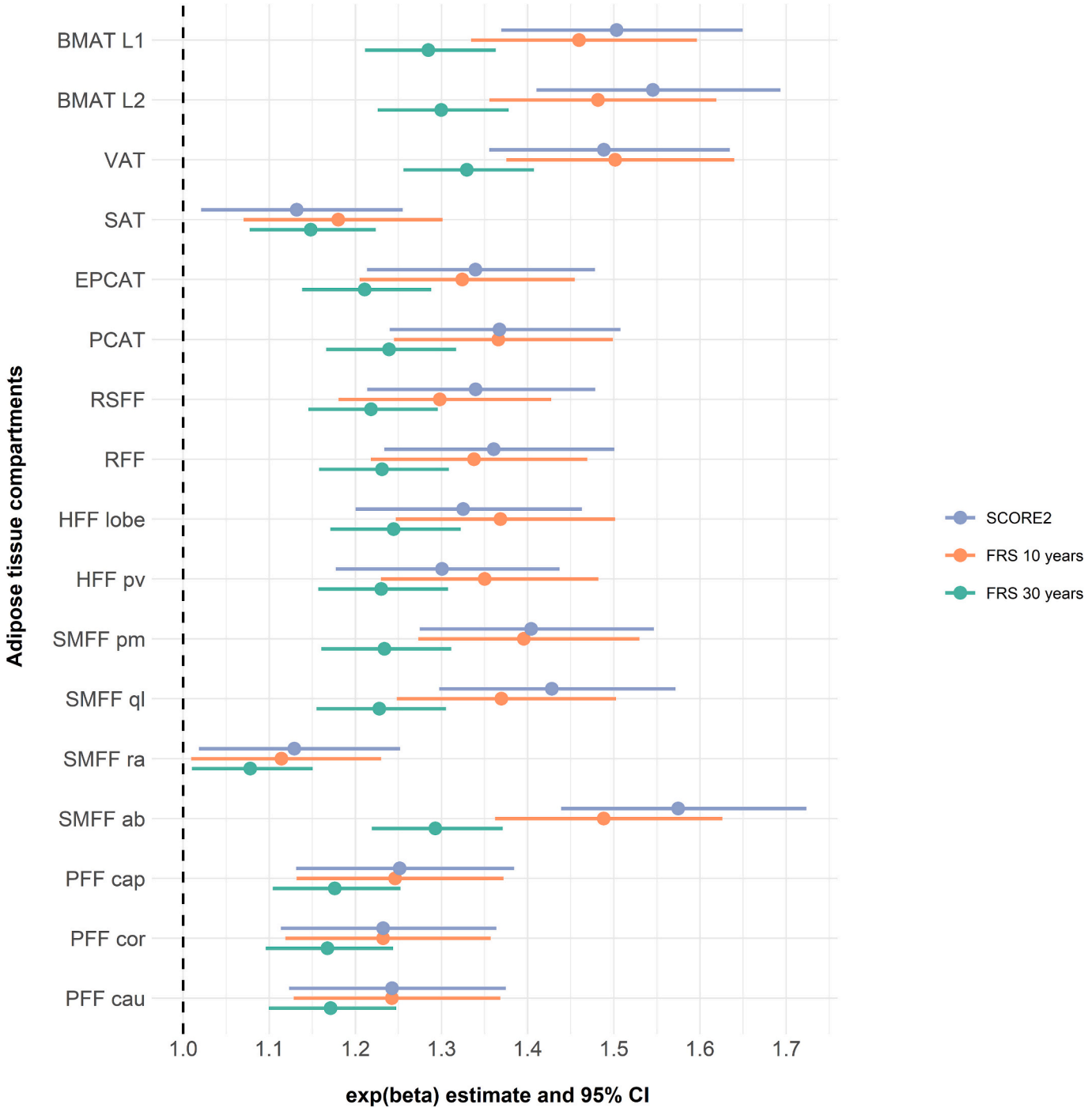

Fig. 2. Association of single adipose tissue compartments with CVD risk scores.
Displayed are exponentiated beta coefficients (corresponding to % change of geometric mean) with corresponding 95%CI from a linear regression model with exposure adipose tissue and outcome log-transformed CVD risk score. Since risk score calculation included age and sex, the regression models were unadjusted. Abbreviations: BMAT L1/L2: bone marrow adipose tissue at vertebrae L1/L2, VAT: visceral adipose tissue, SAT: subcutaneous adipose tissue, EPCAT: epicardial adipose tissue, PCAT: paracardial adipose tissue, RSFF: renal sinus fat fraction, RFF: renal fat fraction, HFF lobe/pv: hepatic fat fraction at right and left lobe or portal vein, SMFF pm/ql/ra/ar: skeletal muscle fat fraction of psoas major/quadratus lumborum/rectus abdominis/autochthonous back muscles, PFF cap/cor/cau: pancreatic fat fraction at caput/corpus/cauda.

subphenotype III, characterized by high muscle and bone marrow fat, whose risk was comparable to a subphenotype V with overall high AT.

By data-driven clustering, we identified five distinct body composition subphenotypes that differed substantially in their fat distribution and cardiometabolic risk profile. The importance of characterizing individual AT distribution patterns beyond BMI has been recognized. In the imaging subsample of the population-based UK Biobank, different body composition profiles based on VAT, SAT, muscle fat and hepatic fat exhibited different degrees of cardiometabolic risks and underline the importance of a multivariable approach to assess body fat distribution [18]. In particular, fatty liver was found to be related to a propensity to diabetes, but not so much to CVD [18]. Furthermore, a study with Japanese participants identified four fat distribution patterns being related to incident T2D cases and replicated the groups with differences

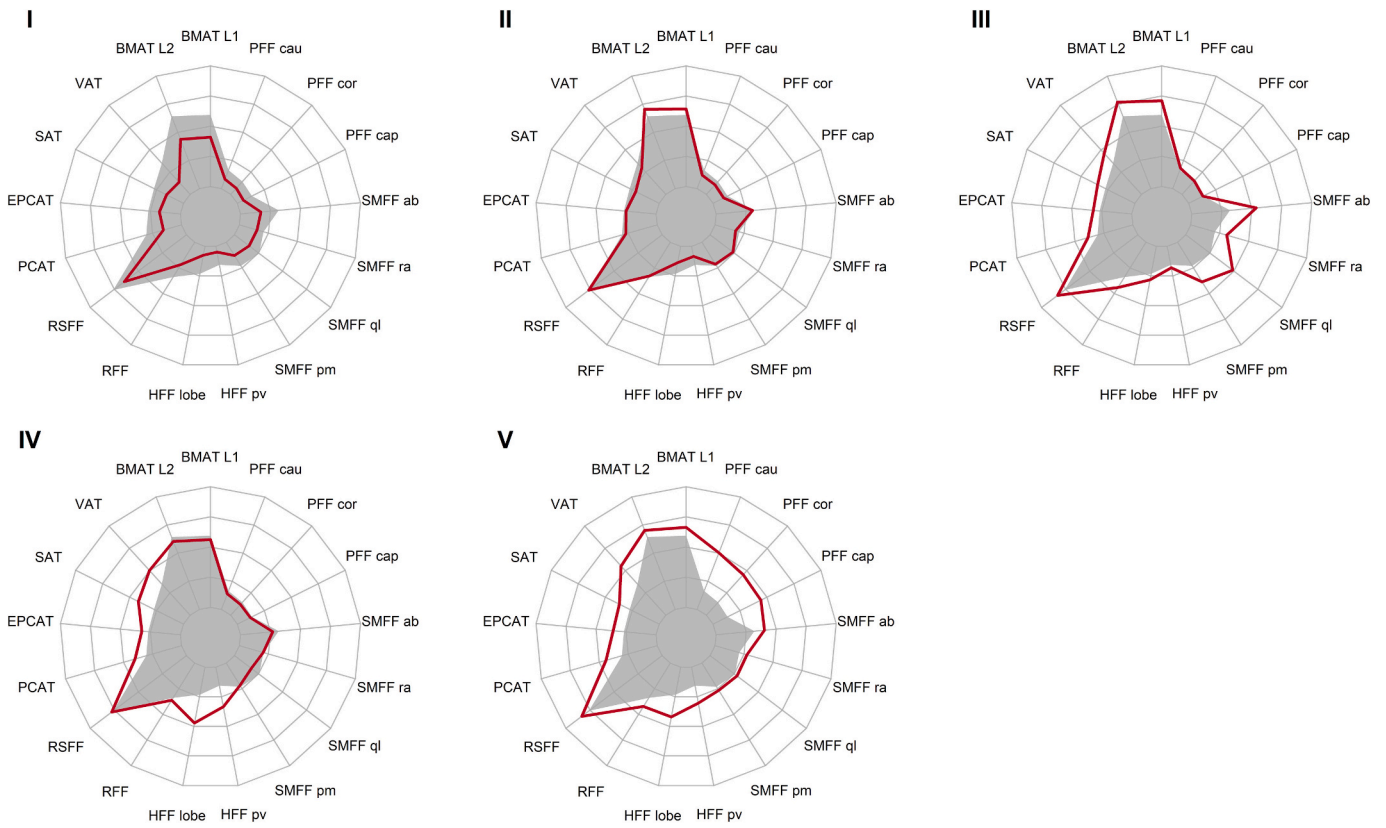

Fig. 3. Five subphenotypes of body composition.
Radar charts of adipose tissue compartments in the five clusters, representing different body composition subphenotypes. Adipose tissue compartments are plotted on min-max-scale. Grey area depicts mean values averaged over the whole sample, red line depicts mean values in the respective clusters. Abbreviations. BMAT L1/L2: bone marrow adipose tissue at vertebrae L1/L2, VAT: visceral adipose tissue, SAT: subcutaneous adipose tissue, EPCAT: epicardial adipose tissue, PCAT: paracardial adipose tissue, RSFF: renal sinus fat fraction, RFF: renal fat fraction, HFF lobe/pv: hepatic fat fraction at right and left lobe or portal vein, SMFF pm/ql/ra/ar: skeletal muscle fat fraction of psoas major/quadratus lumborum/rectus abdominis/autochthonous back muscles, PFF cap/cor/cau: pancreatic fat fraction at caput/corpus/cauda. (For interpretation of the references to colour in this figure legend, the reader is referred to the web version of this article.)

in insulin sensitivity and secretion in German individuals [19].

Associations between individual AT compartments and cardiometabolic risk factors varied greatly. VAT was highly correlated with other AT depots and showed strong associations with CVD risk scores. This agrees with the results from the Framingham Heart Study and the Jackson Heart Study, which identified VAT to be constantly associated with cardiometabolic risk above standard anthropometric indices, but SAT not contributing to cardiometabolic risk above a measure of central obesity [33,34]. VAT, as opposed to SAT, is associated with a higher production of inflammatory cytokines, impaired endocrine function, and insulin resistance [35]. Although excess VAT is established as a cardiometabolic risk factor, recent investigations from the UK Biobank showed that increased muscle fat was more strongly associated with all-cause mortality than VAT [36]. Also in our sample, differences in the profiles were not purely attributable to increase in VAT. On the contrary, variance of VAT was highest in those clusters with high CVD risk, illustrating that individuals with high CVD risk may present substantially different levels of VAT. This underlines the need to shift the focus in body composition profiling beyond abdominal obesity.

The subphenotypes we identified were labeled in ascending order of increasing average VAT and subphenotype I served as reference cluster. Compared to cluster I, individuals in all other clusters had greater CVD risk. Although BMI was only slightly elevated compared to cluster I, the next subphenotype, cluster II, showed a more than doubled CVD risk, mainly conferred by a considerable increase in BMAT and an accompanying increase in LDL cholesterol. Since cluster II had the highest proportion of smokers, our results are in line with the hypothesis that smoking, although at first glance beneficial for weight control, induces an unfavorable AT re-distribution [37].

Subphenotype III was characterized by an increase in all AT compartments, but most strikingly by increased BMAT and skeletal muscle fat. We hypothesize that these characteristics indicate ageing effects, acerbated by a lack of physical activity in this cluster. Sarcopenia, the progressive decline of skeletal muscle function and strength with age, is associated with higher risk of falls, fractures, frailty and mortality [38]. The loss of muscle function is not solely due to decreased muscle mass, but also due to decreased muscle quality, e.g. by increased fatty infiltration of muscle tissue [39]. BIA-derived skeletal muscle mass did not reflect these differences across the clusters, which is in line with prior findings indicating a high prediction error for muscle mass estimation by BIA compared to MRI, particularly in individuals with obesity [26].

A bidirectional relation between sarcopenia and CVD has been described, since both conditions share similar pathophysiological mechanisms including chronic inflammation, insulin resistance and glucose intolerance [40]. The fact that this subphenotype showed high CVD risk in our analysis emphasizes the need to comprehensively assess body composition in the elderly, as single markers are insufficient to characterize age-related changes and associated risks [41]. Particularly, the high amount of postmenopausal women in this cluster underlines the need for additional research on the relation of BMAT, myosteatosis and menopausal status [42], since women are more vulnerable to the "osteosarcopenic obesity" phenotype and associated risks [43].

Interestingly, we found a strong association between BMAT and lipid profile, in particular LDL cholesterol. The role of BMAT in metabolic health is not fully understood so far. Recent studies suggest that it is a fourth type of AT distinct from white, brown, and beige AT, which might

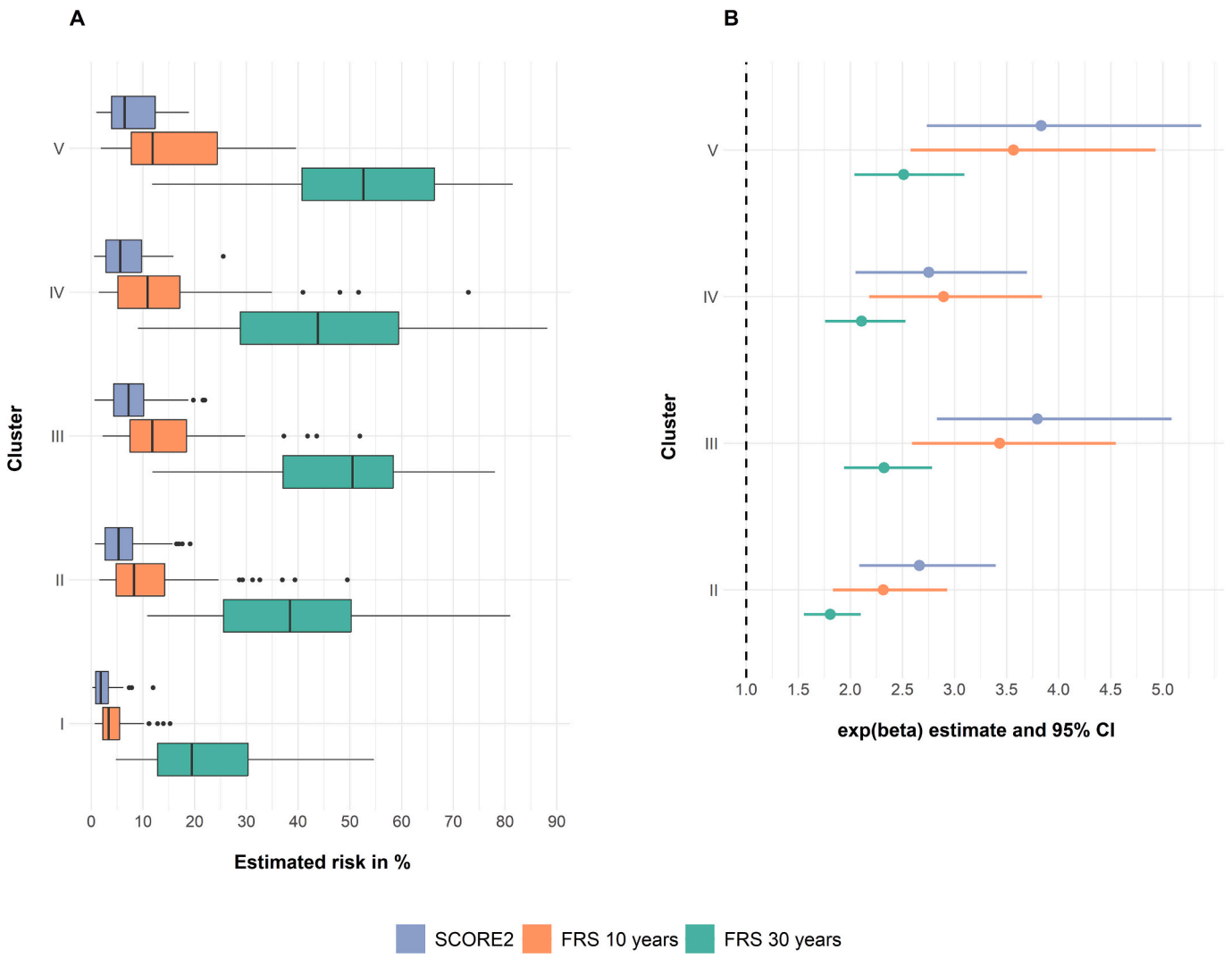

Fig. 4. Association of body composition subphenotypes with CVD risk.
A, left panel: CVD risk, estimated by risk scores (x-axis) in the five body composition subphenotypes (y-axis). B, right panel: Effect estimates (x-axis) of the association of body composition subphenotype (y-axis) with CVD risk. Effect estimates stem from linear regression models with log-transformed risk scores as outcomes and given as exponentiated beta coefficients representing % change of geometric mean. Since risk score calculation included age and sex, the regression models were unadjusted. Cluster I was the reference category.

not only serve as biomarker for bone health but acts as a secretory and metabolically active organ [44,45]. Our results support a distinct role of BMAT, since it was only weakly correlated with other AT compartments, and did not substantially vary with BMI. A positive association between serum lipid levels and BMAT was reported from small studies [46,47] proposing a mechanism of increased BMAT in diabetes patients through hyperlipidemia and promoting marrow adipogenesis, which might underline the association we observed [17].

Although comparably young, cluster IV showed high CVD risk and an unfavorable risk factor profile, including high cholesterol and blood pressure. It was furthermore characterized by a strikingly high hepatic fat content and highest prevalence of hepatic steatosis underlining the link between liver fat and hypertension [11], which we identified in univariate analysis as well. Previous studies suggest systemic inflammation and insulin resistance as potential pathophysiological mechanisms of hypertension as a driver of hepatic steatosis [48]. Our results of increased odds for diabetes in cluster IV corroborate the established association between liver fat and markers of glucose metabolism. Hepatic steatosis and T2D frequently coexist with a suggested bidirectional causal relation [49]. This association might also partly be modulated by VAT, since there is a close connection between VAT and liver fat through drainage of free fatty acids through the portal vein [50]. The high prevalence of overweight and obesity along with highest SAT values in cluster IV further underline this relation. In summary, cluster IV reflects the close interplay between abdominal, hepatic fat and glucose metabolism. However, hepatic steatosis also occurs in individuals without obesity, with an estimated prevalence of 15.5 % among the general population in Europe [5]. We failed to identify a subphenotype clearly corresponding to this “lean fatty liver” phenotype, which might be attributable to our small sample size.

Cluster V presented with an overall high fat content in all considered depots. Most noticeably, pancreatic fat accumulation was strikingly high compared to all other subphenotypes. Additionally, VAT and the proportion of individuals on antidiabetic, antihypertensive or lipid-lowering medication was highest among this cluster. Pancreatic steatosis has been related to the metabolic syndrome in several studies before [14]. Our results underline the hypothesis of fatty pancreas being a manifestation of the metabolic syndrome [51]. However, no pathway has yet been proposed to explain this relation [52]. Additionally, it remains debated whether pancreatic fat accumulation is related to β-cell dysfunction, insulin resistance and T2D [53]. In our analysis, univariate associations were weak, but cluster V showed the highest prevalence of

T2D and the strongest effects regarding HbA1c. Hence, T2D could still be a response to damage of the pancreas caused by fat accumulation in the organ [14]. Further, there was a high prevalence of hepatic steatosis in this subphenotype. The co-occurrence of both pancreatic and hepatic steatosis has been observed before, but possible pathways explaining the relation remain unclear and the relationship might be mediated by central obesity, which is in line with the observed overall obesity in subphenotype V [54].

To address body composition differences between women and men, we compared sex-specific fat distribution patterns of the five subphenotypes. Overall, the observations were consistent with the results described above. However, we constantly found SAT to be more pronounced in women than in men and vice versa for VAT, which is in line with previous studies [55,56], and an even more pronounced increase in muscle fat in women in the higher-risk clusters. Due to the relatively small sample size of our study, we were not able to identify sex-specific subphenotypes, and further account for effects of menopause.

Our study has several limitations. First, the sample size was too small to support more complex analyses, or further relevant stratifications. Second, although our data originate from a population-based study, the imaging sample was a selected subgroup and generalizations to other populations might not be straightforward. Some interesting adipose tissue compartments, such as limb skeletal muscle, which constitutes a large proportion of total body skeletal muscle closely related to glucose metabolism, were not analyzed, since these data were not available from our images.

Moreover, since our data were cross-sectional, we used CVD risk scores to describe the underlying risk factor distribution, which may underestimate true associations with outcomes, since scores can only capture risk conveyed by traditional risk factors. Large longitudinal cohorts with robust outcome ascertainment are needed to not only replicate the body composition subphenotypes, but also evaluate their prognostic ability. Currently, risk prediction based on whole-body MRI is still prohibitively ressource-intensive, which will change with current advances in image reconstruction and image processing.

A major strength of our study are the AT data derived by MRI, which is considered as gold standard for the assessment of fat distribution. Additionally, we included a broad panel of abdominal and ectopic AT measurements, providing a comprehensive characterization of body composition. Lastly, our clustering ansatz to employ an unsupervised, purely data-driven algorithm to identify patterns in body composition enabled a robust and unbiased identification of subphenotypes.

5. Conclusion

Our study demonstrated that body composition profiling using whole-body MRI data is a valid approach to identify distinct, clinically relevant patterns of fat distribution. Subphenotypes of body composition might be superior to single fat compartments in the characterization of cardiometabolic risk, as they better reflect the interplay between different abdominal and ectopic AT depots The usage of whole-body imaging for individualized prevention in clinical practice might become increasingly relevant due to technical advances in data acquisition and faster segmentation. In the context of an opportunistic screening, individualized body composition profiles can be used to complement existing risk assessment strategies and raise awareness for potential treatment. Further research will show if specific non-imaging risk factor profiles are indicative of specific body composition patterns, which could inform personalized lifestyle modifications.

CRediT authorship contribution statement

Elena Grune: Writing – review & editing, Writing – original draft, Visualization, Methodology, Investigation, Formal analysis, Data curation. **Johanna Nattenmüller:** Writing – review & editing, Resources, Investigation. **Lena S. Kiefer:** Writing – review & editing, Resources, Investigation. **Jürgen Machann:** Writing – review & editing, Resources, Investigation. **Annette Peters:** Writing – review & editing, Resources, Investigation, Funding acquisition. **Fabian Bamberg:** Writing – review & editing, Resources, Investigation, Funding acquisition. **Christopher L. Schlett:** Writing – review & editing, Investigation, Funding acquisition. **Susanne Rospleszcz:** Writing – review & editing, Writing – original draft, Supervision, Methodology, Investigation, Data curation, Conceptualization.

Funding

The KORA study was initiated and financed by the Helmholtz Zentrum München–German Research Center for Environmental Health, which is funded by the German Federal Ministry of Education and Research (BMBF) and the state of Bavaria. Data collection in the KORA study is done in cooperation with the University Hospital of Augsburg. Furthermore, KORA research was supported within the Munich Center of Health Sciences (MC-Health), Ludwig-Maximilians-Universität, as part of LMUinnovativ. The KORA MRI sub-study received funding by the German Research Foundation, the Centre for Diabetes Research (DZD e. V., Neuherberg, Germany) and the German Centre for Cardiovascular Disease Research. The KORA-MRI sub-study was supported by an unrestricted research grant from Siemens Healthcare.

Declaration of competing interest

The authors declare that they have no known competing financial interests or personal relationships that could have appeared to influence the work reported in this paper.

Acknowledgements

We thank Prof. Anne-Laure Boulesteix for her helpful advice regarding clustering methods. We thank all participants for their long-term commitment to the KORA study, the staff for data collection and research data management and the members of the KORA Study Group (https://www.helmholtz-munich.de/en/epi/cohort/kora) who are responsible for the design and conduct of the study.

Appendix A. Supplementary data

Supplementary data to this article can be found online at https://doi.org/10.1016/j.metabol.2024.156130.

Data availability

The datasets analyzed during the current study are not publicly available due national data protection laws, since the informed consent given by KORA study participants does not cover data posting in public databases. Data are available upon request by means of a project agreement from KORA. Requests should be sent to kora.passt@helmholtz-munich.de and are subject to approval by the KORA Board. Analysis codes are available from the authors upon reasonable request.

References

[1] Worldwide trends in underweight and obesity from 1990 to 2022: a pooled analysis of 3663 population-representative studies with 222 million children, adolescents, and adults. Lancet 2024;403(10431):1027–50. https://doi.org/10.1016/S0140-6736(23)02750-2.
[2] Endalifer ML, Diress G. Epidemiology, predisposing factors, biomarkers, and prevention mechanism of obesity: a systematic review. J Obes 2020;2020:6134362. https://doi.org/10.1155/2020/6134362.
[3] Blundell JE, Dulloo AG, Salvador J, Frühbeck G. Beyond BMI - phenotyping the obesities. Obes Facts 2014;7(5):322–8. https://doi.org/10.1159/000368783.

[4] Lim S, Meigs JB. Links between ectopic fat and vascular disease in humans. Arterioscler Thromb Vasc Biol 2014;34(9):1820–6. https://doi.org/10.1161/ATVBAHA.114.303035.

[5] Ye Q, Zou B, Yeo YH, Li J, Huang DQ, Wu Y, et al. Global prevalence, incidence, and outcomes of non-obese or lean non-alcoholic fatty liver disease: a systematic review and meta-analysis. Lancet Gastroenterol Hepatol 2020;5(8):739–52. https://doi.org/10.1016/S2468-1253(20)30077-7.

[6] Kahn D, Macias E, Zarini S, Garfield A, Zemski Berry K, MacLean P, et al. Exploring visceral and subcutaneous adipose tissue Secretomes in human obesity: implications for metabolic disease. Endocrinology 2022;163(11). https://doi.org/10.1210/endocr/bqac140.

[7] Rospleszcz S, Dermyshi D, Müller-Peltzer K, Strauch K, Bamberg F, Peters A. Association of serum uric acid with visceral, subcutaneous and hepatic fat quantified by magnetic resonance imaging. Sci Rep 2020:10. https://doi.org/10.1038/s41598-020-57459-z.

[8] Storz C, Heber SD, Rospleszcz S, Machann J, Sellner S, Nikolaou K, et al. The role of visceral and subcutaneous adipose tissue measurements and their ratio by magnetic resonance imaging in subjects with prediabetes, diabetes and healthy controls from a general population without cardiovascular disease. Br J Radiol 2018;91(1089):20170808. https://doi.org/10.1259/bjr.20170808.

[9] Porter SA, Massaro JM, Hoffmann U, Vasan RS, O'Donnel CJ, Fox CS. Abdominal subcutaneous adipose tissue: a protective fat depot? Diabetes Care 2009;32(6):1068–75. https://doi.org/10.2337/dc08-2280.

[10] Chartrand DJ, Murphy-Després A, Alméras N, Lemieux I, Larose E, Després J-P. Overweight, obesity, and CVD risk: a focus on visceral/ectopic fat. Curr Atheroscler Rep 2022;24(4):185–95. https://doi.org/10.1007/s11883-022-00996-x.

[11] Lorbeer R, Bayerl C, Auweter S, Rospleszcz S, Lieb W, Meisinger C, et al. Association between MRI-derived hepatic fat fraction and blood pressure in participants without history of cardiovascular disease. J Hypertens 2017;35(4):737–44. https://doi.org/10.1097/HJH.0000000000001245.

[12] Liu J, Fox CS, Hickson D, Bidulescu A, Carr JJ, Taylor HA. Fatty liver, abdominal visceral fat and cardiometabolic risk factors: the Jackson Heart Study. Arterioscler Thromb Vasc Biol 2011;31(11):2715–22. https://doi.org/10.1161/ATVBAHA.111.234062.

[13] Heber SD, Hetterich H, Lorbeer R, Bayerl C, Machann J, Auweter S, et al. Pancreatic fat content by magnetic resonance imaging in subjects with prediabetes, diabetes, and controls from a general population without cardiovascular disease. PloS One 2017;12(5):e0177154. https://doi.org/10.1371/journal.pone.0177154.

[14] Wagner R, Eckstein SS, Yamazaki H, Gerst F, Machann J, Jaghutriz BA, et al. Metabolic implications of pancreatic fat accumulation. Nat Rev Endocrinol 2022;18(1). https://doi.org/10.1038/s41574-021-00573-3.

[15] Kiefer LS, Fabian J, Rospleszcz S, Lorbeer R, Machann J, Kraus MS, et al. Distribution patterns of intramyocellular and extramyocellular fat by magnetic resonance imaging in subjects with diabetes, prediabetes and normoglycaemic controls. Diabetes Obes Metab 2021;23(8):1868–78. https://doi.org/10.1111/dom.14413.

[16] Bertheau RC, Lorbeer R, Nattenmüller J, Wintermeyer E, Machann J, Linkohr B, et al. Bone marrow fat fraction assessment in regard to physical activity: KORA FF4-3-T MR imaging in a population-based cohort. Eur Radiol 2020;30(6):3417–28. https://doi.org/10.1007/s00330-019-06612-y.

[17] Wu P-H, Joseph G, Saeed I, Pirmoazen AM, Kenny K, Kim TY, et al. Bone marrow adiposity alterations in type 2 diabetes are sex-specific and associated with serum lipid levels. J Bone Miner Res 2023;38(12):1877–84. https://doi.org/10.1002/jbmr.4931.

[18] Linge J, Borga M, West J, Tuthill T, Miller MR, Dumitriu A, et al. Body composition profiling in the UK Biobank imaging study. Obesity (Silver Spring) 2018;26(11):1785–95. https://doi.org/10.1002/oby.22210.

[19] Yamazaki H, Tauchi S, Machann J, Haueise T, Yamamoto Y, Dohke M, et al. Fat distribution patterns and future type 2 diabetes. Diabetes 2022;71(9):1937–45. https://doi.org/10.2337/db22-0315.

[20] Holle R, Happich M, Löwel H, Wichmann HE. KORA–a research platform for population based health research. Gesundheitswesen 2005;67(Suppl. 1):S19–25. https://doi.org/10.1055/s-2005-858235.

[21] Bamberg F, Hetterich H, Rospleszcz S, Lorbeer R, Auweter SD, Schlett CL, et al. Subclinical disease burden as assessed by whole-body MRI in subjects with prediabetes, subjects with diabetes, and normal control subjects from the general population: the KORA-MRI study. Diabetes 2017;66(1). https://doi.org/10.2337/db16-0630.

[22] Qadri S, Vartiainen E, Lahelma M, Porthan K, Tang An, Idilman IS, et al. Marked difference in liver fat measured by histology vs. magnetic resonance-proton density fat fraction: a meta-analysis. JHEP Rep 2024;6(1):100928. https://doi.org/10.1016/j.jhepr.2023.100928.

[23] Singh RG, Yoon HD, Wu LM, Lu J, Plank LD, Petrov MS. Ectopic fat accumulation in the pancreas and its clinical relevance: a systematic review, meta-analysis, and meta-regression. In: Metabolism: Clinical and Experimental; 2017. p. 69. https://doi.org/10.1016/j.metabol.2016.12.012.

[24] Definition and diagnosis of diabetes mellitus and intermediate hyperglycaemia: Report of a WHO/IDF consultation. Geneva, Switzerland: World Health Organization; 2006.

[25] Rospleszcz S, Lorbeer R, Storz C, Schlett CL, Meisinger C, Thorand B, et al. Association of longitudinal risk profile trajectory clusters with adipose tissue depots measured by magnetic resonance imaging. Sci Rep 2019;9(1):16972. https://doi.org/10.1038/s41598-019-53546-y.

[26] Kiefer LS, Fabian J, Rospleszcz S, Lorbeer R, Machann J, Kraus MS, et al. Population-based cohort imaging: skeletal muscle mass by magnetic resonance imaging in correlation to bioelectrical-impedance analysis. J Cachexia Sarcopenia Muscle 2022;13(2):976–86. https://doi.org/10.1002/jcsm.12913.

[27] Janssen I, Heymsfield SB, Baumgartner RN, Ross R. Estimation of skeletal muscle mass by bioelectrical impedance analysis. J Appl Physiol (1985) 2000;89(2):465–71. doi:https://doi.org/10.1152/jappl.2000.89.2.465.

[28] D'Agostino RB, Vasan RS, Pencina MJ, Wolf PA, Cobain M, Massaro JM, et al. General cardiovascular risk profile for use in primary care: the Framingham Heart Study. Circulation 2008;117(6):743–53. https://doi.org/10.1161/CIRCULATIONAHA.107.699579.

[29] Pencina MJ, D'Agostino RB, Larson MG, Massaro JM, Vasan RS. Predicting the thirty-year risk of cardiovascular disease: the Framingham heart study. Circulation 2009;119(24):3078–84. https://doi.org/10.1161/CIRCULATIONAHA.108.816694.

[30] SCORE2-Diabetes: 10-year cardiovascular risk estimation in type 2 diabetes in Europe. Eur Heart J 2023;44(28):2544–56. https://doi.org/10.1093/eurheartj/ehad260.

[31] SCORE2 risk prediction algorithms: New models to estimate 10-year risk of cardiovascular disease in Europe. Eur Heart J 2021;42(25):2439–54. https://doi.org/10.1093/eurheartj/ehab309.

[32] Rospleszcz S, Starnecker F, Linkohr B, von Scheidt M, Gieger C, Schunkert H, et al. Validation of the 30-year Framingham risk score in a German population-based cohort. Diagnostics (Basel) 2022;12(4). https://doi.org/10.3390/diagnostics12040965.

[33] Lee JJ, Pedley A, Hoffmann U, Massaro JM, Levy D, Long MT. Visceral and intrahepatic fat are associated with cardiometabolic risk factors above other ectopic fat depots: the Framingham Heart Study. Am J Med 2018;131(6):684–692.e12. https://doi.org/10.1016/j.amjmed.2018.02.002.

[34] Liu Jiankang, Fox Caroline S, Hickson DeMarc A, May Warren D, Hairston Kristen G, Jeffery Carr J, et al. Impact of abdominal visceral and subcutaneous adipose tissue on cardiometabolic risk factors: the Jackson heart study. J Clin Endocrinol Metab 2010;95(12):5419. https://doi.org/10.1210/jc.2010-1378.

[35] Ibrahim MM. Subcutaneous and visceral adipose tissue: structural and functional differences. Obes Rev 2009;11(1):11–8. https://doi.org/10.1111/j.1467-789X.2009.00623.x.

[36] Jung M, Raghu VK, Reisert M, Rieder H, Rospleszcz S, Pischon T, et al. Deep learning-based body composition analysis from whole-body magnetic resonance imaging to predict all-cause mortality in a large western population. eBioMedicine 2024;110:105467. https://doi.org/10.1016/j.ebiom.2024.105467.

[37] Carrasquilla GD, García-Ureña M, Romero-Lado MJ, Kilpeläinen TO. Estimating causality between smoking and abdominal obesity by Mendelian randomization. Addiction 2024;119(6):1024–34. https://doi.org/10.1111/add.16454.

[38] Cruz-Jentoft AJ, Sayer AA. Sarcopenia. Lancet 2019;393(10191):2636–46. https://doi.org/10.1016/S0140-6736(19)31138-9.

[39] McGregor RA, Cameron-Smith D, Poppitt SD. It is not just muscle mass: a review of muscle quality, composition and metabolism during ageing as determinants of muscle function and mobility in later life. Longev Healthspan 2014;3(1):1–8. https://doi.org/10.1186/2046-2395-3-9.

[40] Damluji AA, Alfaraidhy M, AlHajri N, Rohant NN, Kumar M, Al Malouf C, et al. Sarcopenia and cardiovascular diseases. Circulation 2023;147(20):1534–53. https://doi.org/10.1161/CIRCULATIONAHA.123.064071.

[41] Ponti F, Santoro A, Mercatelli D, Gasperini C, Conte M, Martucci M, et al. Aging and imaging assessment of body composition: from fat to facts. Front Endocrinol (Lausanne) 2020:10. https://doi.org/10.3389/fendo.2019.00861.

[42] Wong AK, Chandrakumar A, Whyte R, Reitsma S, Gillick H, Pokhoy A, et al. Bone marrow and muscle fat infiltration are correlated among postmenopausal women with osteoporosis: the AMBERS cohort study. J Bone Miner Res 2020;35(3):516–27. https://doi.org/10.1002/jbmr.3910.

[43] Conforto R, Rizzo V, Russo R, Mazza E, Maurotti S, Pujia C, et al. Advances in body composition and gender differences in susceptibility to frailty syndrome: role of osteosarcopenic obesity. Metabolism 2024;161:156052. https://doi.org/10.1016/j.metabol.2024.156052.

[44] Suchacki KJ, Tavares AAS, Mattiucci D, Scheller EL, Papanastasiou G, Gray C, et al. Bone marrow adipose tissue is a unique adipose subtype with distinct roles in glucose homeostasis. Nat Commun 2020;11(1):3097. https://doi.org/10.1038/s41467-020-16878-2.

[45] Marinelli Busilacchi E, Morsia E, Poloni A. Bone marrow adipose tissue. Cells 2024;13:9. https://doi.org/10.3390/cells13090724.

[46] Bredella MA, Gill CM, Gerweck AV, Landa MG, Kumar V, Daley SM, et al. Ectopic and serum lipid levels are positively associated with bone marrow fat in obesity. Radiology 2013;269(2):534–41. https://doi.org/10.1148/radiol.13130375.

[47] Slade JM, Coe LM, Meyer RA, McCabe LR. Human bone marrow adiposity is linked with serum lipid levels not T1-diabetes. J Diabetes Complications 2012;26(1):1–9. https://doi.org/10.1016/j.jdiacomp.2011.11.001.

[48] Zhao Y-C, Zhao G-J, Chen Z, She Z-G, Cai J, Li H. Nonalcoholic fatty liver disease: an emerging driver of hypertension. Hypertension 2020;75(2):275–84. https://doi.org/10.1161/HYPERTENSIONAHA.119.13419.

[49] Liu Z, Zhang Y, Graham S, Wang X, Cai D, Huang M, et al. Causal relationships between NAFLD, T2D and obesity have implications for disease subphenotyping. J Hepatol 2020;73(2):263–76. https://doi.org/10.1016/j.jhep.2020.03.006.

[50] Targher G, Corey KE, Byrne CD, Roden M. The complex link between NAFLD and type 2 diabetes mellitus - mechanisms and treatments. Nat Rev Gastroenterol Hepatol 2021;18(9). https://doi.org/10.1038/s41575-021-00448-y.

[51] Sepe PS, Ohri A, Sanaka S, Berzin TM, Sekhon S, Bennett G, et al. A prospective evaluation of fatty pancreas by using EUS. Gastrointest Endosc 2011;73(5):987–93. https://doi.org/10.1016/j.gie.2011.01.015.

[52] Bi Y, Wang J-L, Li M-L, Zhou J, Sun X-L. The association between pancreas steatosis and metabolic syndrome: a systematic review and meta-analysis. Diabetes Metab Res Rev 2019;35(5). https://doi.org/10.1002/dmrr.3142.
[53] Rugivarodom M, Geeratragool T, Pausawasdi N, Charatcharoenwitthaya P. Fatty pancreas: linking pancreas pathophysiology to nonalcoholic fatty liver disease. J Clin Transl Hepatol 2022;10(6):1229–39. https://doi.org/10.14218/JCTH.2022.00085.
[54] Filippatos TD, Alexakis K, Mavrikaki V, Mikhailidis DP. Nonalcoholic fatty pancreas disease: role in metabolic syndrome, "prediabetes," diabetes and atherosclerosis. Dig Dis Sci 2022;67(1):26–41. https://doi.org/10.1007/s10620-021-06824-7.
[55] Schorr M, Dichtel LE, Gerweck AV, Valera RD, Torriani M, Miller KK, et al. Sex differences in body composition and association with cardiometabolic risk. Biology of Sex Differences 2018;9(1). https://doi.org/10.1186/s13293-018-0189-3.
[56] de Ritter R, Sep SJS, van Greevenbroek MMJ, Kusters, Yvo HAM, Vos RC, et al. Sex differences in body composition in people with prediabetes and type 2 diabetes as compared with people with normal glucose metabolism: the Maastricht Study. Diabetologia 2023;66(5):861–72. https://doi.org/10.1007/s00125-023-05880-0.